Innovative Approaches to Antenna Characterization: A Compressive Sensing Framework

M. Salucci, N. Anselmi, and A. Massa

2024/04/12

ELEDIA Research Center

Contents

ELEDIA Research Center

1 Magnitude Failure Factor and Phase Shift values impact on the Near Field Error

1.1 Test performed using the parameters : $\mathbf{M} = 25$, $\mathbf{F}^{(\mathbf{s})} = 7$ and $\mathbf{P}^{(\mathbf{s})} = 5$

By using a number of :

- simulated configurations to build the over-complete basis :
  - number of failure factors, $\mathbf{F}^{(\mathbf{s})} = 7$;
  - number of phase shifts, $\mathbf{P}^{(\mathbf{s})} = 5$;
- measurement points, $\mathbf{M} = 25$;

the objective of this section is to verify if the near-field error has a relation with the value of the failure (either in magnitude or in phase) or if it is completely insensitive to the failure intensity.

ELEDIA Research Center

1.1.1 *AUT* with only a magnitude failure affecting the 3^{rd} row ($\nu^{(3)} = [0,\, 0.15,\, 0.45,\, 0.65,\, 1]$); incremented failure ranges to build the over-complete basis ($\nu^{(s)} \in [0.0,\, 1.0]\,,\; F^{(s)} = 7, \gamma^{(s)} \in [-\pi,\, \pi]\,,\; P^{(s)} = 5$) and $\mathbf{M = 25}$

Parameters

Gold Antenna (Without Defects)

- Geometry : Planar array of microstrip patches on the (x, y) plane;
- Working Frequency : $f = 3.6\,[GHz]$ ($\lambda = 83.27 \times 10^{-3}\,[m]$ in free space);
- Substrate (PEC-backed) :
  - Dimensions : infinite;
  - Relative Permittivity : $\varepsilon_{r,sub} = 4.7$;
  - Loss Tangent : $tan\,\delta_{sub} = 0.014$;
  - Thickness : $h_{sub} = 0.019\,[\lambda]$ $(1.6\,[mm])$;
- Microstrip patches :
  - Dimensions : $l_x \approx 0.22\,[\lambda]$ $(18.16\;[mm])$, $l_y \approx 0.33\,[\lambda]$ $(27.25\;[mm])$;
  - Feeding : pin-fed;
- Spacing between elements : $d_x = d_y = \frac{\lambda}{2}$;
- Number of elements in each row : $N_x = 6$;
- Number of elements in each column : $N_y = 10$;
- Total number of elements : $N = (N_x \times N_y) = 60$;
- Total size of the antenna : $L_x = 5\,[\lambda]$, $L_y = 9\,[\lambda]$;
- Element excitations : $w_n^{(s)} = 1.0 + j0.0$, $n = 1, ..., N^{(s)}$, $s = 1, ..., S$;

Antenna Under Test (AUT - With Defects)

1. Failures of the excitation magnitude of the 3^{rd} row;
   - Magnitude failure of the elements in the 3^{rd} row ($s = 3$) : $\nu^{(3)} = [0,\, 0.15,\, 0.45,\, 0.65,\, 1]$;

ELEDIA Research Center

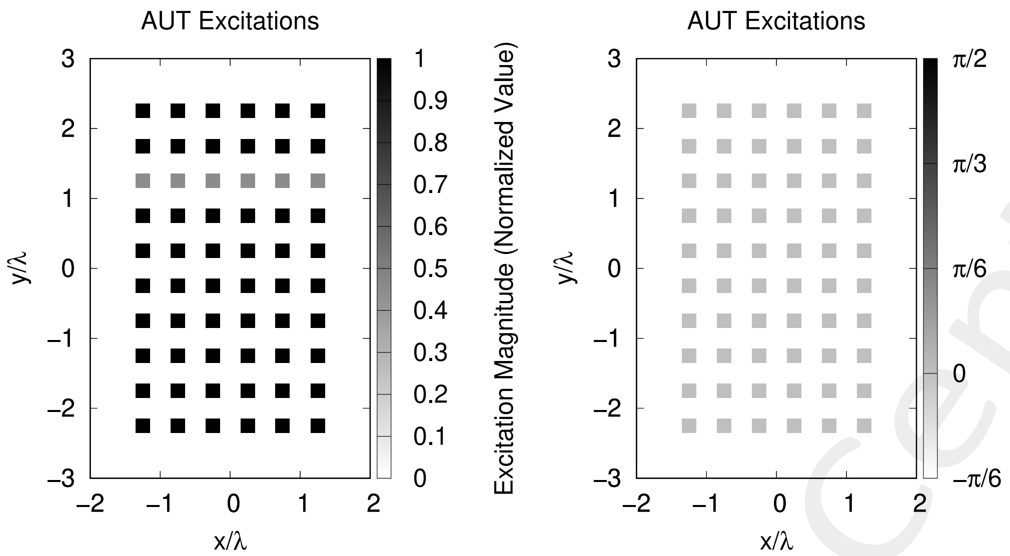

(*a*) (*b*)

Figure 1: (*a*) Magnitude of the element excitations in the *AUT* (e.g. $\nu^{(3)} = 0.45$), (*b*) phase of the element excitations in the *AUT* .

Measurement Set-Up

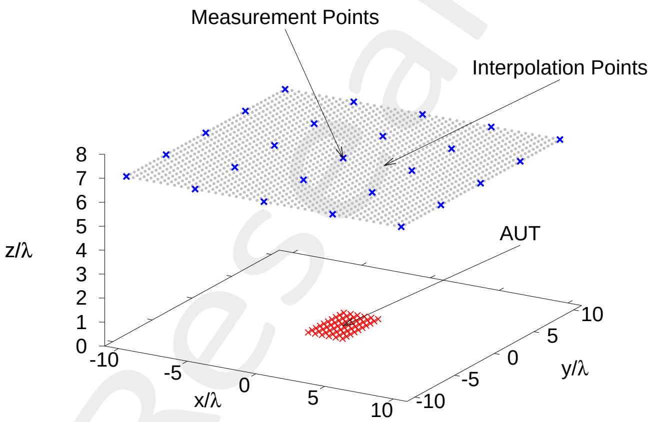

Figure 2: Disposition of the interpolation points ($T = 1681$) and of the measurement points (M=25) in the near-field region of the *AUT*.

- Type of measurements : near-field;
- Height of the measurement region : $H = 7\,[\lambda]$;
- Interpolation points :
  - Number of points : $T = 41 \times 41 = 1681$;
  - Coordinates : $x_t \in [-10,\,10]\,[\lambda],\ y_t \in [-10,\,10]\,[\lambda],\ z_t = H\,[\lambda],\ t = 1, ..., T$;
  - Interpolation step : $\Delta_{x/y}^{int} = 0.5\,[\lambda]$;
- Measurement points :
  - Coordinates : $x_m^{meas} \in [-10,\,10]\,[\lambda],\ y_m^{meas} \in [-10,\,10]\,[\lambda],\ z_m^{meas} = H\,[\lambda],\ m = 1, ..., M$;

ELEDIA Research Center

- Number of points : $M = 25$;
- Measurement step : $\Delta_{x/y}^{meas} = 5\,[\lambda]$
- Ratio between number of measurements and total number of elements : $(M/N) = 0.42$;

Measurement-by-Design Technique

- Number of generated bases : $B = 20$;
- Bases $b = 1, ..., 10$: magnitude failures in each row $(s = 1, ..., 10)$
  - Failure factor of the elements : $\nu^{(s)} = [0.0,\ 1.0],\ \ s = 1, ..., 10$;
  - Number of simulated failure factors : $F^{(s)} = 7,\ s = 1, ..., 10$;
- Bases $b = 11, ..., 20$: phase failures in each row $(s = 1, ..., 10)$
  - Phase shift of the elements : $\gamma^{(s)} \in [-\pi,\ \pi]\,[rad],\ \ s = 1, ..., 10$;
  - Number of simulated phase shifts: $P^{(s)} = 5,\ s = 1, .., 10$;
- Threshold on the singular values magnitude (normalized) : $\eta = -40\,[dB]$;
- Total number of simulated AUT configurations : $K = S \times (F^{(s)} + P^{(s)}) = 10 \times (7 + 5) = 120$;

Dimension of the Over-Complete Basis

The dimension of the over-complete basis is

$$Q = 40$$

This number is given by the sum of the vectors belonging to the two considered bases:

1. Magnitude failures : $Q_1, ..., Q_{10} = 2$;
2. Phase failures : $Q_{11}, ..., Q_{20} = 2$.

Alternative (*BCS*) MbD parameters

- Toleration factor for *BCS* solver: $Tolerance = 1 \times 10^{-8}$;
- Initial noise variance for *BCS* solver: $\eta_0^{opt_1} = 10^{-2}$. This value has been obtained as a result of a calibration procedure;

Original (*OMP*) MbD parameters

- Max. number of iterations of the OMP algorithm : $I = \{1;\ 2;\ 3;\ ...;\ 10\}$;
- Selected iteration to report the results: depends on the particular considered case.

Noise

- SNR on the measured data : $SNR = \{50;\ 40;\ 30;\ 20;\ 10\}\,[dB]$;
- Noise seed : $Noise\_Seed = 11$.

ELEDIA Research Center

Near-Field vs Magnitude Failure Factor ($\nu^{(3)}$)

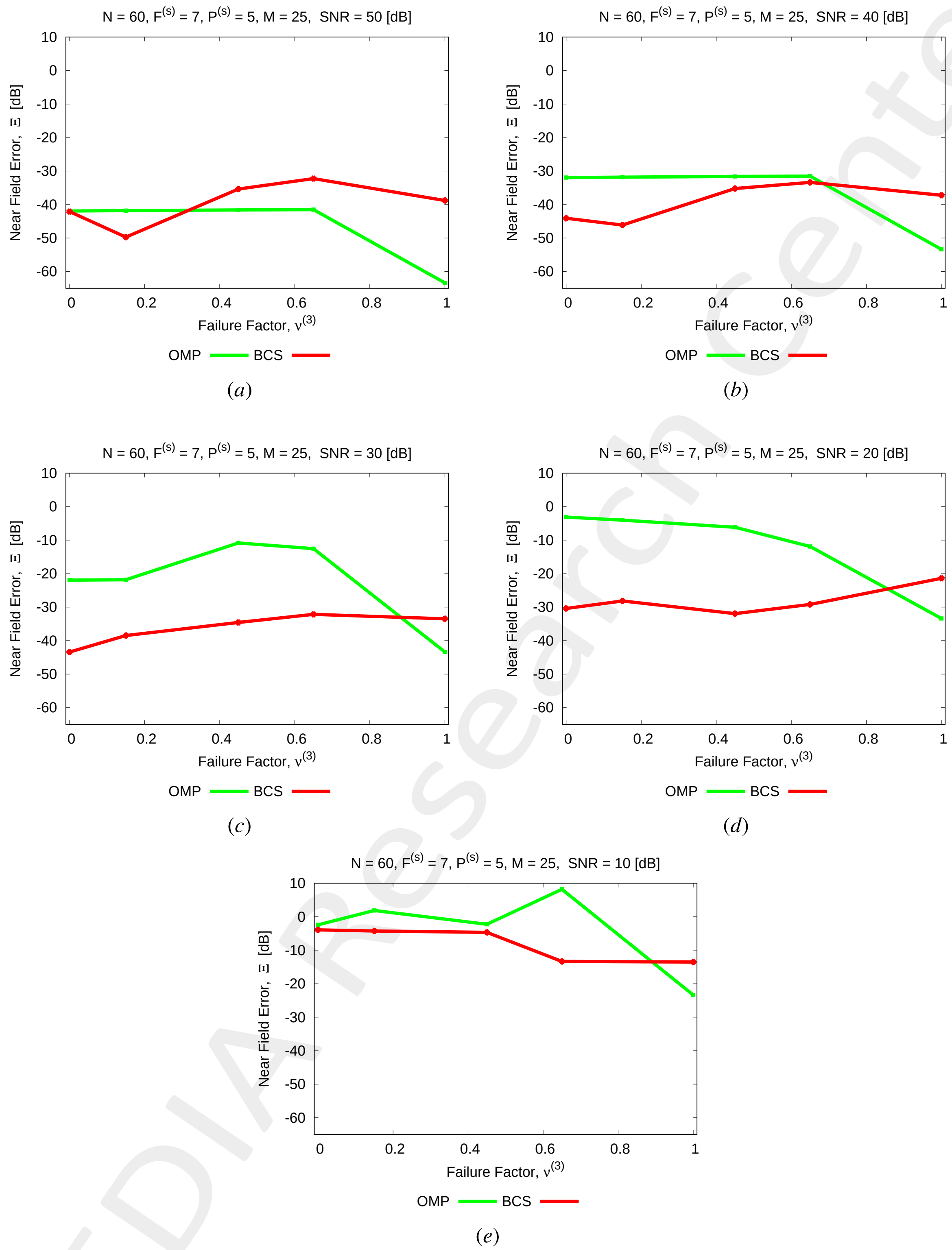

Figure 3: Behaviour of the near-field matching error, Ξ, as a function of the magnitude failure factor affecting the 3^{rd} row of the *AUT*, $\nu^{(3)}$: (*a*) $SNR = 50\,[dB]$, (*b*) $SNR = 40\,[dB]$, (*c*) $SNR = 30\,[dB]$, (*d*) $SNR = 20\,[dB]$, (*e*) $SNR = 10\,[dB]$

Comments

The reported results show that:

ELEDIA Research Center

- the *OMP* solver is quite insensitive to the variation of the magnitude failure factor (the curve is almost flat) except when the magnitude failure is very low (note: higher the value of $\nu^{(s)}$ and more the *AUT* behaves like the *Gold* antenna); indeed, for $\nu^{(3)} \geq 0.65$, it is possible to observe an important error decrease of about $20\,[dB]$ or more. This is true for all the considered SNR values;

- the near-field error of the *BCS* algorithm, even if there are some small variations of the resulting curve, appears to be more independent from the variation of the magnitude failure factor than the *OMP* solver; indeed, whatever the SNR value, the error variation is always less than $10\,[dB]$.

ELEDIA Research Center

1.1.2 *AUT* with only a phase failure affecting the 3^{rd} row ($\gamma^{(3)} = [-180,\,-150,\,-45,\,0,\,60,\,135,\,180]\,[Deg]$); incremented failure ranges to build the over-complete basis ($\nu^{(s)} \in [0.0,\,1.0]\,,\; F^{(s)} = 7$, $\gamma^{(s)} \in [-\pi,\,\pi]\,,\; P^{(s)} = 5$) and $\mathrm{M} = \mathbf{25}$

Parameters

Gold Antenna (Without Defects)

- Geometry : Planar array of microstrip patches on the (x, y) plane;
- Working Frequency : $f = 3.6\,[GHz]$ ($\lambda = 83.27 \times 10^{-3}\,[m]$ in free space);
- Substrate (PEC-backed) :
  - Dimensions : infinite;
  - Relative Permittivity : $\varepsilon_{r,sub} = 4.7$;
  - Loss Tangent : $tan\,\delta_{sub} = 0.014$;
  - Thickness : $h_{sub} = 0.019\,[\lambda]$ $(1.6\,[mm])$;
- Microstrip patches :
  - Dimensions : $l_x \approx 0.22\,[\lambda]$ $(18.16\;[mm])$, $l_y \approx 0.33\,[\lambda]$ $(27.25\;[mm])$;
  - Feeding : pin-fed;
- Spacing between elements : $d_x = d_y = \frac{\lambda}{2}$;
- Number of elements in each row : $N_x = 6$;
- Number of elements in each column : $N_y = 10$;
- Total number of elements : $N = (N_x \times N_y) = 60$;
- Total size of the antenna : $L_x = 5\,[\lambda]$, $L_y = 9\,[\lambda]$;
- Element excitations : $w_n^{(s)} = 1.0 + j0.0,\; n = 1, ..., N^{(s)},\; s = 1, ..., S$;

Antenna Under Test (AUT - With Defects)

1. Failures of the excitation phase of the 3^{rd} row;
   - Phase shift of the elements in the 3^{rd} row ($s = 3$) : $\gamma^{(3)} = [-\pi, -\frac{5}{6}\pi,\, -\frac{\pi}{4},\, 0,\, \frac{\pi}{3},\, \frac{3}{4}\pi,\, \pi]\,[rad]$;

ELEDIA Research Center

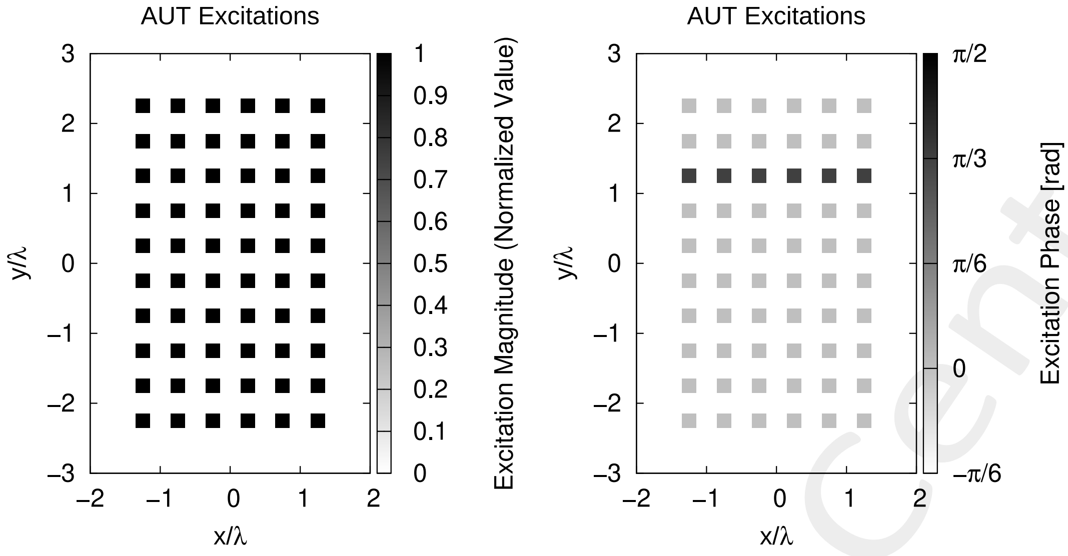

(*a*) (*b*)

Figure 4: (*a*) Magnitude of the element excitations in the *AUT* , (*b*) phase of the element excitations in the *AUT* (e.g. $\gamma^{(3)} = \frac{\pi}{3}\,[rad]$) .

Measurement Set-Up

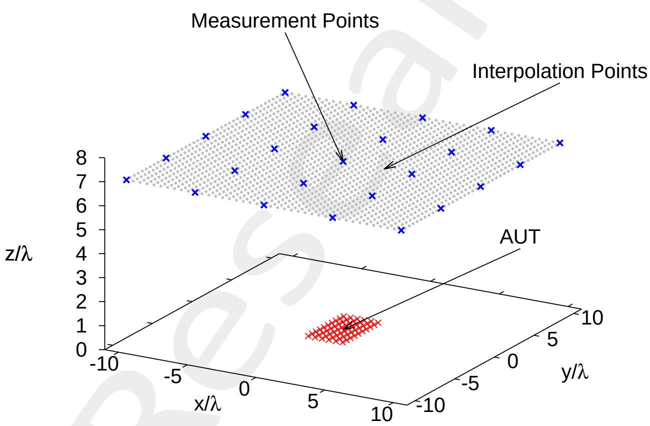

Figure 5: Disposition of the interpolation points ($T = 1681$) and of the measurement points ($M = 25$) in the near-field region of the *AUT.*

- Type of measurements : near-field;
- Height of the measurement region : $H = 7\,[\lambda]$;
- Interpolation points :
  - Number of points : $T = 41 \times 41 = 1681$;
  - Coordinates : $x_t \in [-10,\, 10]\,[\lambda],\ y_t \in [-10,\, 10]\,[\lambda],\ z_t = H\,[\lambda],\ t = 1, ..., T$;
  - Interpolation step : $\Delta^{int}_{x/y} = 0.5\,[\lambda]$;
- Measurement points :
  - Coordinates : $x^{meas}_m \in [-10,\, 10]\,[\lambda],\ y^{meas}_m \in [-10,\, 10]\,[\lambda],\ z^{meas}_m = H\,[\lambda],\ m = 1, ..., M$;

ELEDIA Research Center

- Number of points : $M = 25$;
- Measurement step : $\Delta_{x/y}^{meas} = 5\,[\lambda]$
- Ratio between number of measurements and total number of elements : $(M/N) = 0.42$;

Measurement-by-Design Technique

- Number of generated bases : $B = 20$;
- Bases $b = 1, ..., 10$: magnitude failures in each row $(s = 1, ..., 10)$
  - Failure factor of the elements : $\nu^{(s)} = [0.0,\ 1.0],\ \ s = 1, ..., 10$;
  - Number of simulated failure factors : $F^{(s)} = 7,\ s = 1, ..., 10$;
- Bases $b = 11, ..., 20$: phase failures in each row $(s = 1, ..., 10)$
  - Phase shift of the elements : $\gamma^{(s)} \in [-\pi,\ \pi]\,[rad],\ \ s = 1, ..., 10$;
  - Number of simulated phase shifts: $P^{(s)} = 5,\ s = 1, .., 10$;
- Threshold on the singular values magnitude (normalized) : $\eta = -40\,[dB]$;
- Total number of simulated AUT configurations : $K = S \times (F^{(s)} + P^{(s)}) = 10 \times (7 + 5) = 120$;

Dimension of the Over-Complete Basis

The dimension of the over-complete basis is

$$Q = 40$$

This number is given by the sum of the vectors belonging to the two considered bases:

1. Magnitude failures : $Q_1, ..., Q_{10} = 2$;
2. Phase failures : $Q_{11}, ..., Q_{20} = 2$.

Alternative (*BCS*) MbD parameters

- Toleration factor for *BCS* solver: $Tolerance = 1 \times 10^{-8}$;
- Initial noise variance for *BCS* solver: $\eta_0^{opt_1} = 10^{-2}$. This value has been obtained as a result of a calibration procedure;

Original (*OMP*) MbD parameters

- Max. number of iterations of the OMP algorithm : $I = \{1;\ 2;\ 3;\ ...;\ 10\}$;
- Selected iteration to report the results: depends on the particular considered case.

Noise

- SNR on the measured data : $SNR = \{50;\ 40;\ 30;\ 20;\ 10\}\,[dB]$;
- Noise seed : $Noise\_Seed = 63$.

ELEDIA Research Center

Near-Field vs Phase Shift Factor ($\gamma^{(3)}$)

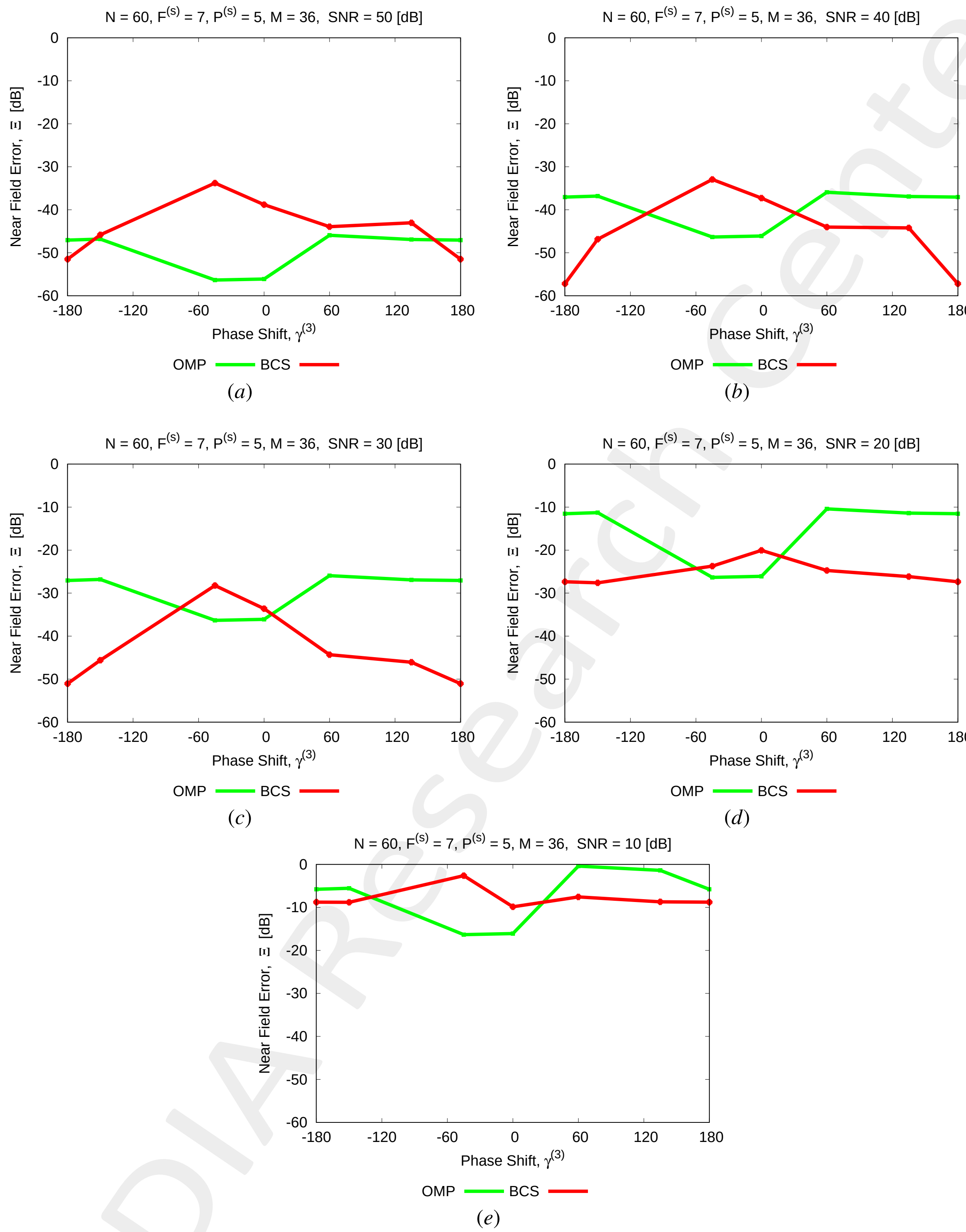

Figure 6: Behaviour of the near-field matching error, Ξ, as a function of the phase shift factor affecting the 3^{rd} row of the *AUT*, $\gamma^{(3)}$: (*a*) $SNR = 50\,[dB]$, (*b*) $SNR = 40\,[dB]$, (*c*) $SNR = 30\,[dB]$, (*d*) $SNR = 20\,[dB]$, (*e*) $SNR = 10\,[dB]$

Comments

The reported results show a slight dependence of the near-field error of both *OMP* and *BCS* solver. The phase shift factors of main interest are those in the middle of the considered range; in particular, the performance of the two algorithms are different because:

ELEDIA Research Center

- the *OMP* solver reaches the minimum error for $\gamma^{(3)} = -65\,[Deg]$ and $\gamma^{(3)} = 0\,[Deg]$ (the latter case corresponds to the situation in which the AUT has no defects) which results in a resulting curve valley at those points;
- on the contrary, the *BCS* algorithm, at $\gamma^{(3)} = -65\,[Deg]$ and $\gamma^{(3)} = 0\,[Deg]$, obtains its higher error so that its resulting curve presents a peak at those points.

ELEDIA Research Center

More information on the topics of this document can be found in the following list of references.

References

[1] M. Salucci, N. Anselmi, M. D. Migliore and A. Massa, "A bayesian compressive sensing approach to robust near-field antenna characterization," *IEEE Trans. Antennas Propag.*, vol. 70, no. 9, pp. 8671-8676, Sep. 2022 (DOI: 10.1109/TAP.2022.3177528).

[2] B. Li, M. Salucci, W. Tang, and P. Rocca, "Reliable field strength prediction through an adaptive total-variation CS technique," *IEEE Antennas Wirel. Propag. Lett.*, vol. 19, no. 9, pp. 1566-1570, Sep. 2020.

[3] M. Salucci, M. D. Migliore, P. Rocca, A. Polo, and A. Massa, "Reliable antenna measurements in a near-field cylindrical setup with a sparsity promoting approach," *IEEE Trans. Antennas Propag.*, vol. 68, no. 5, pp. 4143-4148, May 2020.

[4] G. Oliveri, M. Salucci, N. Anselmi, and A. Massa, "Compressive sensing as applied to inverse problems for imaging: theory, applications, current trends, and open challenges," *IEEE Antennas Propag. Mag. - Special Issue on "Electromagnetic Inverse Problems for Sensing and Imaging*," vol. 59, no. 5, pp. 34-46, Oct. 2017.

[5] A. Massa, P. Rocca, and G. Oliveri, "Compressive sensing in electromagnetics - A review," *IEEE Antennas Propag. Mag.*, pp. 224-238, vol. 57, no. 1, Feb. 2015.

[6] A. Massa and F. Texeira, "Guest-Editorial: Special Cluster on Compressive Sensing as Applied to Electromagnetics," *IEEE Antennas Wirel. Propag. Lett.*, vol. 14, pp. 1022-1026, 2015.

[7] G. Oliveri, N. Anselmi, M. Salucci, L. Poli, and A. Massa, "Compressive sampling-based scattering data acquisition in microwave imaging," *J. Electromagn. Waves Appl*, vol. 37, no. 5, 693-729, March 2023 (DOI: 10.1080/09205071.2023.2188263).

[8] G. Oliveri, L. Poli, N. Anselmi, M. Salucci, and A. Massa, "Compressive sensing-based Born iterative method for tomographic imaging," *IEEE Trans. Microw. Theory Techn.*, vol. 67, no. 5, pp. 1753-1765, May 2019.

[9] M. Salucci, L. Poli, and G. Oliveri, "Full-vectorial 3D microwave imaging of sparse scatterers through a multi-task Bayesian compressive sensing approach," *J. Imaging*, vol. 5, no. 1, pp. 1-24, Jan. 2019.

[10] M. Salucci, A. Gelmini, L. Poli, G. Oliveri, and A. Massa, "Progressive compressive sensing for exploiting frequency-diversity in GPR imaging," *J. Electromagn. Waves Appl.*, vol. 32, no. 9, pp. 1164-1193, 2018.

[11] N. Anselmi, L. Poli, G. Oliveri, and A. Massa, "Iterative multi-resolution bayesian CS for microwave imaging," *IEEE Trans. Antennas Propag.*, vol. 66, no. 7, pp. 3665-3677, Jul. 2018.

[12] N. Anselmi, G. Oliveri, M. A. Hannan, M. Salucci, and A. Massa, "Color compressive sensing imaging of arbitrary-shaped scatterers," *IEEE Trans. Microw. Theory Techn.*, vol. 65, no. 6, pp. 1986-1999, Jun. 2017.

ELEDIA Research Center

[13] N. Anselmi, G. Oliveri, M. Salucci, and A. Massa, “Wavelet-based compressive imaging of sparse targets” *IEEE Trans. Antennas Propag.*, vol. 63, no. 11, pp. 4889-4900, Nov. 2015.

[14] G. Oliveri, P.-P. Ding, and L. Poli, “3D crack detection in anisotropic layered media through a sparseness-regularized solver,” *IEEE Antennas Wirel. Propag. Lett.*, vol. 14, pp. 1031-1034, 2015.

[15] L. Poli, G. Oliveri, P.-P. Ding, T. Moriyama, and A. Massa, “Multifrequency Bayesian compressive sensing methods for microwave imaging,” *J. Opt. Soc. Am. A*, vol. 31, no. 11, pp. 2415-2428, 2014.

[16] G. Oliveri, N. Anselmi, and A. Massa, “Compressive sensing imaging of non-sparse 2D scatterers by a total-variation approach within the Born approximation,” *IEEE Trans. Antennas Propag.*, vol. 62, no. 10, pp. 5157-5170, Oct. 2014.

[17] L. Poli, G. Oliveri, F. Viani, and A. Massa, “MT-BCS-based microwave imaging approach through minimum-norm current expansion,” *IEEE Trans. Antennas Propag.*, vol. 61, no. 9, pp. 4722-4732, Sep. 2013.

[18] F. Viani, L. Poli, G. Oliveri, F. Robol, and A. Massa, “Sparse scatterers imaging through approximated multitask compressive sensing strategies,” *Microwave Opt. Technol. Lett.*, vol. 55, no. 7, pp. 1553-1558, Jul. 2013.

[19] L. Poli, G. Oliveri, P. Rocca, and A. Massa, “Bayesian compressive sensing approaches for the reconstruction of two-dimensional sparse scatterers under TE illumination,” *IEEE Trans. Geosci. Remote Sensing*, vol. 51, no. 5, pp. 2920-2936, May 2013.

[20] P. Rocca, N. Anselmi, M. A. Hannan, and A. Massa, “Conical frustum multi-beam phased arrays for air traffic control radars,” *Sensors*, vol. 22, no. 19, 7309, pp. 1-18, 2022 (DOI: 10.3390/s22197309)

[21] F. Zardi, G. Oliveri, M. Salucci, and A. Massa, “Minimum-complexity failure correction in linear arrays via compressive processing,” *IEEE Trans. Antennas Propag.*, vol. 69, no. 8, pp. 4504-4516, Aug. 2021.

[22] N. Anselmi, G. Gottardi, G. Oliveri, and A. Massa, “A total-variation sparseness-promoting method for the synthesis of contiguously clustered linear architectures,” *IEEE Trans. Antennas Propag.*, vol. 67, no. 7, pp. 4589-4601, Jul. 2019.

[23] M. Salucci, A. Gelmini, G. Oliveri, and A. Massa, “Planar arrays diagnosis by means of an advanced Bayesian compressive processing,” *IEEE Trans. Antennas Propag.*, vol. 66, no. 11, pp. 5892-5906, Nov. 2018.

[24] L. Poli, G. Oliveri, P. Rocca, M. Salucci, and A. Massa, “Long-Distance WPT Unconventional Arrays Synthesis,” *J. Electromagn. Waves Appl.*, vol. 31, no. 14, pp. 1399-1420, Jul. 2017.

[25] G. Oliveri, M. Salucci, and A. Massa, “Synthesis of modular contiguously clustered linear arrays through a sparseness-regularized solver,” *IEEE Trans. Antennas Propag.*, vol. 64, no. 10, pp. 4277-4287, Oct. 2016.

[26] M. Carlin, G. Oliveri, and A. Massa, “Hybrid BCS-deterministic approach for sparse concentric ring isophoric arrays,” *IEEE Trans. Antennas Propag.*, vol. 63, no. 1, pp. 378-383, Jan. 2015.

[27] G. Oliveri, E. T. Bekele, F. Robol, and A. Massa, “Sparsening conformal arrays through a versatile BCS-based method,” *IEEE Trans. Antennas Propag.*, vol. 62, no. 4, pp. 1681-1689, Apr. 2014.

ELEDIA Research Center

[28] F. Viani, G. Oliveri, and A. Massa, “Compressive sensing pattern matching techniques for synthesizing planar sparse arrays,” *IEEE Trans. Antennas Propag.*, vol. 61, no. 9, pp. 4577-4587, Sept. 2013.

[29] P. Rocca, M. A. Hannan, M. Salucci, and A. Massa, “Single-snapshot DoA estimation in array antennas with mutual coupling through a multi-scaling BCS strategy,” *IEEE Trans. Antennas Propag.*, vol. 65, no. 6, pp. 3203-3213, Jun. 2017.

[30] M. Carlin, P. Rocca, G. Oliveri, F. Viani, and A. Massa, “Directions-of-arrival estimation through Bayesian Compressive Sensing strategies,” *IEEE Trans. Antennas Propag.*, vol. 61, no. 7, pp. 3828-3838, Jul. 2013.

[31] M. Carlin, P. Rocca, G. Oliveri, and A. Massa, “Bayesian compressive sensing as applied to directions-of-arrival estimation in planar arrays," *J. Electromagn. Waves Appl.*, vol.2013, pp.1-12, 2013 (DOI :10.1155/2013/245867).

ELEDIA Research Center